

**NMR determination of the partial density of states and of the electronic correlation in  $\text{Mg}_{1-x}\text{Al}_x\text{B}_2$** 

S. Serventi, G. Allodi, C. Bucci, R. De Renzi, and G. Guidi

*Dipartimento di Fisica e Istituto Nazionale di Fisica della Materia, Università di Parma, I-43100 Parma, Italy*

E. Pavarini

*Dipartimento di Fisica "A. Volta" e Istituto Nazionale di Fisica della Materia, Università di Pavia, I-27100 Pavia, Italy*

P. Manfrinetti and A. Palenzona

*Dipartimento di Chimica e Istituto Nazionale di Fisica della Materia, Università di Genova, I-16146 Genova, Italy*

(Received 4 December 2002; published 17 April 2003)

We measured the  $^{27}\text{Al}$  and  $^{11}\text{B}$  NMR spin lattice relaxation rates and the isotropic Knight shifts in powder samples of  $\text{Mg}_{1-x}\text{Al}_x\text{B}_2$ . The comparison with band structure calculations allows the experimental determination of the partial DOS and its dependence upon the Al concentration  $x$ . Agreement is obtained for its absolute values as well as for its behavior upon doping. The satisfactory understanding of the electronic wave function around the probe nuclei validates our determination of a surprisingly large Korringa ratio, from the comparison between  $^{27}\text{Al}$  relaxations and shifts, which can only partially be attributed to Al disorder.

DOI: 10.1103/PhysRevB.67.134518

PACS number(s): 74.70.Ad, 74.25.Jb, 74.62.Dh, 76.60.-k

Superconductivity at  $T_c = 39$  K in  $\text{MgB}_2$  is undoubtedly an example of phonon mediated pairing.<sup>1-3</sup> The detailed origin of the remarkably high transition temperature is still a matter of debate, in which both more standard<sup>2,3</sup> as well as less conventional<sup>4</sup> views are held. Material science and correlated electron physics are confronted with a simple lattice in which band calculations are extremely reliable. It is therefore important to find accurate experimental tests for the basic electronic properties, to be compared with theory.

According to state-of-art electronic structure calculations based on density functional theory in the local (spin) density approximation [L(S)DA], two kinds of bands  $\pi$  and  $\sigma$  cross the Fermi surface, hence contribute to the normal and superconductive properties. The low-dimensional hole character of the  $\sigma$  bands, with Fermi energy  $E_F$  close to its bottom at  $\Gamma$ ,<sup>2,5</sup> together with the large energy of the anharmonic  $E_{2g}$  (Ref. 1) boron modes are probably key features.

The investigation of the well characterized alloy  $\text{Mg}_{1-x}\text{Al}_x\text{B}_2$  (Refs. 6-8)—where the  $\sigma$  bands are completely filled around  $x=0.5$  and at the same composition  $T_c$  drops to zero—can validate our understanding of the electronic structure and of the mechanism of superconductivity. The presence of Al has two effects: the smaller ionic radius of Al vs Mg contracts the lattice axially (as shown by the inset of Fig. 1), and the substitution of  $\text{Al}^{+3}$  for  $\text{Mg}^{+2}$  induces electron doping.

In the present work we measure the NMR relative Knight frequency shift  $K$  and the spin lattice relaxation rate  $T_1^{-1}$  in  $\text{Mg}_{1-x}\text{Al}_x\text{B}_2$ . In addition, we perform first-principles calculations for the same quantities and compare our data with the theoretical results. NMR studies of normal<sup>9</sup> and superconducting state properties<sup>10</sup> have been performed in the pure material, and the opening of the gap was investigated<sup>11</sup> also on  $\text{Mg}_{1-x}\text{Al}_x\text{B}_2$ . Our NMR experiments probe selected partial density of states (DOS) at the Fermi level ( $E_F$ ), via the nuclear hyperfine interactions, thus providing a unique chance of testing the electronic structure of  $\text{Mg}_{1-x}\text{Al}_x\text{B}_2$  in the normal state. We show that all the partial density of states

decrease with increasing  $x$  up to  $x=0.4$ . We find excellent agreement between experimental and theoretical dependence of  $1/T_1 T$  and  $K$  upon Al concentration. Finally we determine the  $^{27}\text{Al}$  Korringa ratio  $1/T_1 T K^2$ , which ought to be a universal constant for free electrons, and find a larger value, by a factor 2, whereas LSDA band structure<sup>14</sup> predicts a 10% reduction.

The Hamiltonian describing the nuclear hyperfine interaction with conduction electrons, may be written as follows (we neglect the small spin-orbit coupling):

$$\mathcal{H}_{hf} = \mu_0 \gamma_n \gamma_e \hbar^2 \mathbf{I} \cdot \left[ \frac{8\pi}{3} \delta(\mathbf{r}) \mathbf{S} + \frac{3(\mathbf{S} \cdot \hat{r}) \hat{r} - \mathbf{S}}{r^3} + \frac{\mathbf{I}}{r^3} \right], \quad (1)$$

where  $\mathbf{S}$  and  $\mathbf{I}$  are the electronic and nuclear spin operator,  $\gamma_e$  and  $\gamma_n$  their gyromagnetic ratios,  $\mathbf{I}$  is the electron orbital momentum operator, and  $\mathbf{r}$  the electron coordinate relative to the nucleus. The first two terms in Eq. (1) are the Fermi contact and the dipole-dipole interaction. The third term is the coupling with the electronic orbital momentum. The two quantities accessible from the experiment,  $K$  and  $1/T_1$ , are respectively the static average and the time dependent effect of the perturbation, given by Eq. (1), on the Zeeman spin Hamiltonian.<sup>12</sup>

Standard treatment of this interaction<sup>12,14</sup> shows that both the Knight shift and the relaxation rate can be written as powers of linear combinations of projected DOS at the Fermi level  $N_{lm}(E_F)$  ( $l, m$  are eigenvalues of  $\mathbf{I}_z$ ;  $E_F$  is omitted hereafter). The Fermi contact interaction contributes to  $K$  and  $T_1^{-1}$  through the  $s$ -wave component  $N_s = N_{00}$ . The dipole-dipole and the orbital terms contribute through combinations of  $N_{lm}$  components with  $l > 0$  (the  $l=1$  ones dominate for  $\text{Mg}_{1-x}\text{Al}_x\text{B}_2$ ).

The first principles results presented here are based on the TB LMTO-ASA method (Stuttgart LMTO47 code).<sup>13</sup> The theoretical approach used to calculate the NMR quantities were

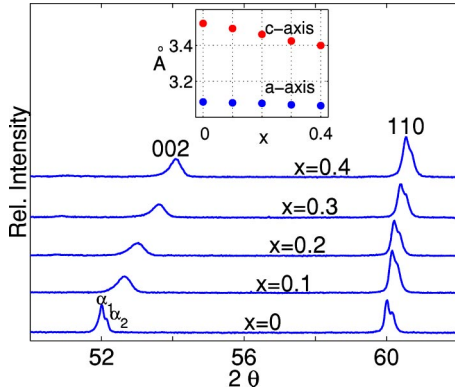


FIG. 1. A portion of the x-ray powder pattern from  $\text{Mg}_{1-x}\text{Al}_x\text{B}_2$  ( $\text{Cu}K_{\alpha_1}$ ) showing the [002] and [110] peaks.

described in full detail in Ref. 14. The dependence of  $1/T_1T$  and  $K$  upon electron doping is studied in the rigid bands approximation.

Powders were obtained by the standard procedure, reacting 99.98% Mg, 99.97% Al in stoichiometric proportions inside a Ta vessel at  $1000^\circ\text{C}$  for 150 h. The x-ray powder patterns reveal single phase materials at all compositions (Fig. 1), contrary to earlier reports<sup>8</sup> on samples obtained with much shorter reaction times. Transition temperatures and  $c$ -axis contractions agree with literature data.<sup>6,7</sup> For both  $^{27}\text{Al}$  ( $I=5/2$ ,  $^{27}\gamma/2\pi=11.094$  MHz/T) and  $^{11}\text{B}$  ( $I=3/2$ ,  $^{11}\gamma/2\pi=13.660$  MHz/T) we report shifts and relaxations of the central  $1/2 \leftrightarrow -1/2$  transition of the quadrupole-split spectra, measured in an external field of about 7 T. Relaxation rates were measured with an aperiodic saturation sequence of hard pulses, which determines the full saturation of the complete quadrupolar spectrum and hence a single exponential recovery law  $I(t)=I_0(1-e^{-t/T_1})$ . Typical results for the two nuclei are shown as  $\ln[1-I(t)/I_0]$  in Fig. 2. We obtain the same rates from experiments where the sole central line is irradiated.

The isotropic Knight shift  $K_{\text{iso}}=\text{Tr}(K)$  is determined by comparison with standard references tri-ethylborane (TEB) (chemical shift  $\sigma=-18$  ppm) for  $^{11}\text{B}$  and  $\text{AlCl}_3 \cdot 6\text{H}_2\text{O}$  ( $\sigma=0$  ppm) for  $^{27}\text{Al}$ . A conservative errorbar on  $K_{\text{iso}}$  is estimated as  $1/5$  of the linewidth (due to dipole-dipole interactions<sup>9</sup>), divided by the Larmor frequency.

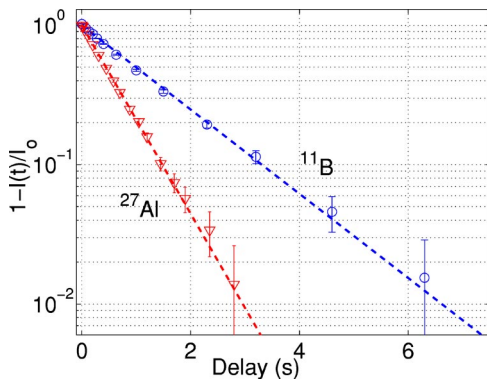


FIG. 2. Single exponential saturation recovery for the  $x=0.3$  sample:  $^{11}\text{B}$  open symbols;  $^{27}\text{Al}$  filled symbols.

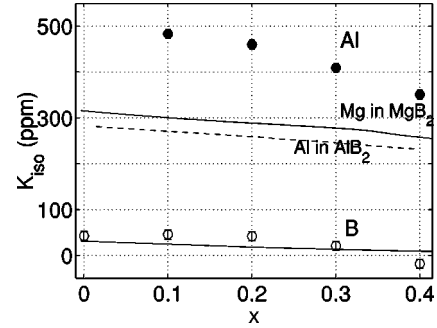


FIG. 3. Isotropic Knight shift for  $^{11}\text{B}$  (open symbol) and  $^{27}\text{Al}$  (filled symbol) versus Al concentration  $x$ . Lines refer to theoretical values for  $K_{\text{iso}}$  calculated for B, Mg, in  $\text{MgB}_2$  and for Al in  $\text{AlB}_2$ .

Figure 3 shows the measured  $K_{\text{iso}}$  as a function of  $x$  (symbols), together with the theoretical curves. The experimental value of  $^{11}K_{\text{iso}}(0)=43(10)$  ppm for boron in the pure compound agrees within errorbars with the precise MAS determination of Ref. 9, and only within the order of magnitude with the values reported by other authors.<sup>10</sup> We measure a value of  $-18(10)$  ppm at  $x=0.4$ , close to that obtained<sup>9</sup> in pure  $\text{AlB}_2$ . This small negative value is practically zero, almost within errorbars (if not directly due to a very small chemical shift contribution, common to all compositions). Hence the data show a progressive reduction of the B  $s$ -projected density of states, which nearly vanishes at  $x=0.4$ , and it is in very good agreement with the solid curve, which represents the total theoretical  $K_{\text{iso}}$  for B, obtained with the *ab initio* spin susceptibility, and including also the small core polarization term, evaluated at  $x=0$ . We neglect the Van Vleck contribution to  $K$  (both for B and for Al) since for  $p$ -band metals<sup>15,16</sup> it is small and it nearly cancels with the diamagnetic term.

Figure 3 also shows the Al data, together with two theoretical curves: one is  $K_{\text{iso}}$  for Mg in the electron doped rigid  $\text{MgB}_2$  and the other is  $K_{\text{iso}}$  for Al in the hole doped rigid  $\text{AlB}_2$ . The two curves are very similar, and were both obtained by using the *ab initio* spin susceptibility. They lie well below the experimental data, suggesting that a larger spin susceptibility should be used in order to explain the Al data.

The Korringa relaxation rate may be written as

$$\frac{1}{T_1} = 2\pi k_B \hbar \gamma_n^2 \sum_{\mathbf{q}} |A(\mathbf{q})|^2 \frac{\chi''(\mathbf{q}, \omega)}{\omega} \quad (2)$$

with  $A(\mathbf{q})$  a nuclear structure factor (a constant for the on site Fermi interaction under appropriate conditions), and the imaginary part  $\chi''$  of the spin susceptibility at the Larmor frequency  $\omega$  is another measure of the DOS. For both nuclei the  $1/T_1$  data display the simple Korringa linear temperature dependence expected for metals<sup>12</sup> down to the superconducting transition, hence  $(T_1T)^{-1}$  is constant with  $T$ . Our  $^{11}\text{B}$  value in pure  $\text{MgB}_2$  for this Korringa constant is  $8.0(2) \times 10^{-3}(\text{s K})^{-1}$ , in agreement with published values. For  $^{27}\text{Al}$  we measure  $0.115(5)$  and  $0.100(2)(\text{s K})^{-1}$  at  $x=0.1$  and  $x=0.2$ , respectively.

Figures 4(a) and 4(b) shows the square root of the measured Korringa constant at a given  $x$  value, divided by the

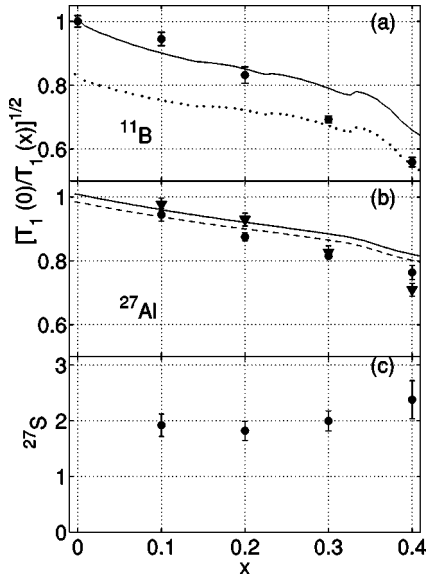


FIG. 4.  $1/\sqrt{T_1(x)}$  data (circles) normalized to its  $x=0$  value together with theoretical lines (full line for total, dashed and dotted for the contact and orbital contribution, respectively) for (a)  $^{11}\text{B}$  and (b)  $^{27}\text{Al}$  where normalized  $K_{\text{iso}}$  data (triangles) are also shown. (c) Deviation factor for  $^{27}\text{Al}$  vs  $x$  (see text).

corresponding quantity at  $x=0$ , for  $^{11}\text{B}$  and  $^{27}\text{Al}$ , respectively (circles). For the  $^{27}\text{Al}$  data the normalization is extrapolated linearly from the two smallest Al concentrations. The lines are the corresponding theoretical results, renormalized to the  $x=0$  value. The relaxation rate, following Eq. (1), is the sum of three independent terms.<sup>14</sup> Pavarini *et al.*<sup>14</sup> demonstrate that the ratio of the contact contribution [proportional to square of the wave function at the nucleus  $|\Phi_0(0)|^2$ ] to the dipolar and orbital contributions (proportional to the expectation value  $\langle r^{-3} \rangle$ ) can be evaluated by the square of the factors

$${}^nR(x) = \frac{2|\Phi_0(0)|^2 N_s(x)}{3\langle r^{-3} \rangle_{11} N_p(x)}, \quad (3)$$

where  $N_s$  and  $N_p$  are the total  $s$ ,  $p$  projected DOS for a given atom. The following numbers were reported<sup>9,14</sup> from first-principles calculations  ${}^{11}R(0)=0.35$ ,  ${}^{25}R(0)=5$  (for  $^{25}\text{Mg}$ ),  ${}^{11}R(1)=2.3$ , and  ${}^{27}R(1)=16$ .

For  $^{11}\text{B}$  at  $x=0$   ${}^{11}R(0)=0.35$  dictates that the dominant contribution is the orbital term (dotted curve in Fig. 4), three times larger than the dipole-dipole term and ten times larger than the contact term. With increasing  $x$  the Fermi level moves toward the top of the Fermi  $\sigma$  bands and the microscopic mechanism which controls the  $^{11}\text{B}$  relaxation changes drastically, from predominantly orbital at  $x=0$  to mostly contact at  $x=1$  (in agreement with experiments<sup>9</sup>). Figure 4 shows that the total value (solid curve) decreases with  $x$  mainly because the (dominant) orbital term is decreasing.

The value of  ${}^{25}R(0)=5$  indicates that the contact contribution to the  $^{25}\text{Mg}$  relaxation rate dominates over the dipolar and orbital term<sup>9,14</sup> in  $\text{MgB}_2(x=0)$ . A similar behavior is expected also for Al, which replaces Mg in  $\text{Mg}_{1-x}\text{Al}_x\text{B}_2$ .

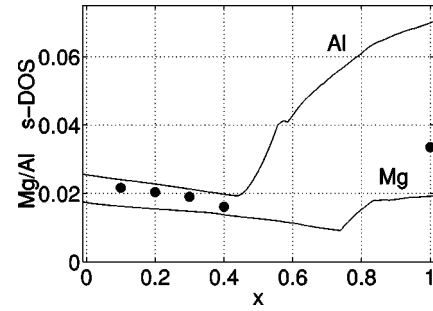


FIG. 5.  $N_s$  DOS for  $\text{MgB}_2$  and for  $\text{AlB}_2$ , together with the  ${}^{27}(T_1T)^{-1/2}$  experimental data (symbols) arbitrarily rescaled at  $x=0.1$ .

The value of  ${}^{27}R(1)=16$  suggests that Al and Mg detect essentially Fermi contact interactions for all concentrations. If this is the case then both  $K_{\text{iso}}(x)$  and  $\sqrt{1/T_1(x)T}$  are proportional to the same projected DOS  $N_s(x)$ . This is directly confirmed by Fig. 4(b), where normalized Knight shift data (triangles) are also plotted. The agreement among the two sets of data and the calculated behavior is excellent.

The experimental values<sup>9</sup> of both the relaxation rate constant and the shift in  $\text{AlB}_2$  are larger than in our low doping samples  $({}^{27}T_1T)^{-1}=2.2[{}^{27}T_1(x=0)T]^{-1}$  and  ${}^{27}K_{\text{iso}}=1.9{}^{27}K_{\text{iso}}(x=0)$ . Therefore the partial  $s$ -wave DOS at Al must have a minimum between  $x=0.4$  and  $x=1$ . In Fig. 5 we show the  $\text{MgB}_2$  and  $\text{AlB}_2$   $N_s$  density of states as a function of  $N_e - 8 \equiv x$ , where  $N_e$  is the total number of electrons ( $N_e=8$  for  $x=0$ ), together with the  ${}^{27}\text{Al}$   $\sqrt{(1/T_1)T}$  data, arbitrarily rescaled. Both curves do show the expected minimum.

Thus the Knight shifts (Fig. 3) and the square roots of the Korringa constants (Fig. 4) determine experimentally the behavior of the partial density of states as a function of doping: the B and the Al Knight shifts give their respective  $s$ -projected DOS, the square root of  $1/{}^{27}T_1T$  gives again the Al  $s$ -projected DOS, and finally, since the orbital and the dipole-dipole contribution to the B Korringa ratio are proportional<sup>14</sup> to the square of the B  $p$  DOS,  $N_{1m}$  and for B  $N_x=N_y \sim N_z \sim N_p/3$ , the square root of  $1/{}^{11}T_1T$  gives  $N_p$ , the B  $p$ -projected DOS.

Since the Al NMR data is dominated by  $N_s$  we may extract a reliable experimental determination of the Korringa ratio  $(T_1T)^{-1}K_{\text{iso}}^{-2}$ , which is equal to a universal constant  $C_0=4\pi k_B(\gamma_e/\gamma_n)^2/\hbar$ , for noninteracting electrons with a Pauli spin susceptibility  $\chi_0$ . Deviations of the quantity  ${}^nS=1/{}^nT_1T({}^nK_{\text{iso}})^2C_0$  from the value 1 are due to departures of the susceptibility  $\chi$  from  $\chi_0$ . Figure 4(c) shows the rather large deviation  ${}^{27}S \sim 2$  measured for  $^{27}\text{Al}$ . The modifications of the free electron susceptibility are quite generally of the form  $G(\mathbf{q}, \omega)=\chi/\chi_0=1/[1-I(\mathbf{q})\chi_0(\mathbf{q}, \omega)]$ . Similar correction factors were evidenced by recent de Haas van Alphen measurements.<sup>18</sup> Electron correlations of ferromagnetic type [ $\chi(\mathbf{q})$  enhanced around  $\mathbf{q}=0$ ] imply correction by the Stoner factor  $I(0)>0$ . A (Knight shift) enhancement factor for  $\chi_0(\mathbf{0}, 0)$ ,  $G(0)=1.33$ , is obtained from LSDA calculations,<sup>14</sup> in qualitative agreement with  ${}^{11}K_{\text{iso}}$  data up to  $x=0.4$  (Fig. 3), and in quantitative agreement with the experimental<sup>9</sup>

value of  $^{25}\text{S}$  for  $^{25}\text{Mg}$ . The relaxation rate, however, requires  $G(\mathbf{q})$  and if a Lindhart form is assumed for the  $\mathbf{q}$ -dependent spin susceptibility the combined effect of these LSDA Stoner factors yields a deviation  $^{27}\text{S}=0.9$ , not compatible with the values of Fig. 4(c).

Shastry *et al.* showed<sup>17</sup> that disorder may produce a large deviation from  $\chi_0$  of the same sign as the experimental one. The disorder effect on  $^{27}\text{S}$  may be quantified from Ref. 17, Fig. 3: our experimental values for  $0.1 \leq x \leq 0.4$  match those of the figure for a carrier mean free path  $l$  in the range  $1 < l < 3$  (in units of the inverse Fermi wave vector  $k_F^{-1}$ ). An estimate of  $l$  from the resistivity<sup>19</sup>  $\rho$  yields  $lk_F = \sqrt[3]{12\pi^2} \hbar r_s / e^2 \rho = 88, 39, 33$ , respectively, for  $x = 0, 0.05, 0.1$ . The experimental value of  $l$  for  $x = 0.1$  is incompatible with that required by Ref. 17. Although disorder definitely contributes to the  $^{27}\text{S}$  value, further departures from  $\chi_0$  must be considered, such as the presence of peaks in  $\chi(\mathbf{q})$  for  $\mathbf{q} \neq 0$  [e.g., antiferromagnetic (AF-) type correlations], which may lead to an increase of  $^{27}\text{S}$ . We speculate

that, if a minor tendency towards AF correlations is indeed present in the pure material, the *impurity* Al might enhance it, by means of its independent charge and spin screening densities, in a mechanism akin to Ruderman-Kittel-Kasuya-Yosida<sup>20</sup> oscillations. After submission we learnt that a similar work is reported by Papavassiliou *et al.*<sup>21</sup>

In conclusion, the measurement of nuclear relaxations and shifts on two distinct lattice sites in  $\text{Mg}_{1-x}\text{Al}_x\text{B}_2$  yields the variation of partial densities of states, which agree with the trend obtained from LSDA calculation. This indicates that the electronic structure of  $\text{MgB}_2$  obtained within LSDA is basically reliable. However, a surprisingly large value of the Korringa ratio for Al is found indicating combined effects of disorder and local modifications of the spin susceptibility.

This work was done under an INFM PRA UMBRA grant. We acknowledge Dr. C. Vignali for technical assistance, the partial use of Centro Interdipartimentale Misure, and useful discussions with F. Borsa and S. Massidda.

- 
- <sup>1</sup>R. Osborn, E. A. Goremychkin, A. I. Kolesnikov, and D. G. Hinks, *Phys. Rev. Lett.* **87**, 017005 (2001).
- <sup>2</sup>J. Kortus, I. I. Mazin, K. D. Belashchenko, V. P. Antropov, and L. L. Boyer, *Phys. Rev. Lett.* **86**, 4656 (2001).
- <sup>3</sup>T. Yildirim, O. Gülseren, J. W. Lynn, C. M. Brown, T. J. Udovic, Q. Huang, N. Rogado, K. A. Regan, M. A. Hayward, J. S. Slusky, T. He, M. K. Haas, P. Khalifah, K. Inumaru, and R. Cava, *Phys. Rev. Lett.* **87**, 037001 (2001).
- <sup>4</sup>E. Cappelluti, S. Ciuchi, C. Grimaldi, L. Pietronero, and S. Strässler, *Phys. Rev. Lett.* **88**, 117003 (2002).
- <sup>5</sup>G. Satta, G. Profeta, F. Bernardini, A. Continenza, and S. Massidda, *Phys. Rev. B* **64**, 104507 (2001).
- <sup>6</sup>A. Bianconi, S. Agrestini, D. Di Castro, G. Campi, G. Zangari, N. L. Saini, A. Saccone, S. De Negri, M. Giovannini, G. Profeta, A. Continenza, G. Satta, S. Massidda, A. Cassetta, A. Pifferi, and M. Colapietro, *Phys. Rev. B* **65**, 174515 (2002).
- <sup>7</sup>O. de la Peña, A. Aguayo, and R. de Coss, *Phys. Rev. B* **66**, 012511 (2002).
- <sup>8</sup>J. S. Slusky, N. Rogado, K. A. Regan, M. A. Hayward, P. Khalifah, T. He, K. Inumaru, S. Louriéro, M. K. Haas, H. W. Zandbergen, and R. J. Cava, *Nature (London)* **410**, 343 (2001).
- <sup>9</sup>H. Baek, B. J. Suh, E. Pavarini, F. Borsa, R. G. Barnes, S. L. Bud'ko, and P. C. Canfield, *Phys. Rev. B* **66**, 104510 (2002).
- <sup>10</sup>H. Kotegawa, K. Ishida, Y. Kitaoka, T. Muranaka, and J. Akimitsu, *Phys. Rev. Lett.* **87**, 127001 (2001).
- <sup>11</sup>H. Kotegawa, K. Ishida, Y. Kitaoka, T. Muranaka, N. Nakagawa, H. Takagiwa, and J. Akimitsu, *Phys. Rev. B* **66**, 064516 (2002).
- <sup>12</sup>C. P. Slichter, *Principles of Magnetic Resonance* (Springer, New York, 1990).
- <sup>13</sup>O. K. Andersen, Z. Pawłowska, and O. Jepsen, *Phys. Rev. B* **34**, 5253 (1986).
- <sup>14</sup>E. Pavarini and I. I. Mazin, *Phys. Rev. B* **64**, 140504 (2001).
- <sup>15</sup>R.H. Hammond and G.M. Kelly, *Phys. Rev. Lett.* **18**, 156 (1967).
- <sup>16</sup>L. H. Chou and T. J. Rowland, *Phys. Rev. B* **45**, 11 580 (1992).
- <sup>17</sup>B. S. Shastry and E. Abrahams, *Phys. Rev. Lett.* **72**, 1933 (1994).
- <sup>18</sup>E. A. Yelland, J. R. Cooper, A. Carrington, N. E. Hussey, P. J. Meeson, S. Lee, A. Yamamoto, and S. Tajima, *Phys. Rev. Lett.* **88**, 217002 (2002).
- <sup>19</sup>B. Lorenz, R. L. Meng, Y. Y. Xue, and C. W. Chu, *Phys. Rev. B* **64**, 052513 (2001).
- <sup>20</sup>M. A. Ruderman and C. Kittel, *Phys. Rev.* **96**, 99 (1954); T. Kasuya, *Prog. Theor. Phys.* **16**, 45 (1956); K. Yosida, *Phys. Rev.* **106**, 893 (1957).
- <sup>21</sup>G. Papavassiliou, M. Pissas, M. Karayanni, M. Fardis, S. Koutandos, and K. Prassides, *Phys. Rev. B* **66**, 140514(R) (2002).